ELSEVIER

Journal of Power Sources 68 (1997) 30–36

JOURNAL OF POWER SOURCES

Electrolyte solutions for anodes in rechargeable lithium batteries

Yoshiharu Matsuda [a,*], Masayuki Morita [b], Masashi Ishikawa [b]

[a] *Department of Applied Chemistry, Faculty of Engineering, Kansai University, 3-3-35 Yamate-Cho, Suita 564, Japan*

[b] *Department of Applied Chemistry and Chemical Engineering, Faculty of Engineering, Yamaguchi University, 2557 Tokiwadai, Ube 755, Japan*

Accepted 27 December 1996

Abstract

The suitability of organic electrolyte systems for highly graphitized carbon anodes has been discussed by considering the stability of co-solvents included in ethylene carbonate-based electrolytes and the stability of lithium salts. The side-reaction and the film formation on the graphitized anodes were found to affect the discharge capacity of the graphitized anodes. With respect to the lithium salts, lithium bistrifluoromethylsulfonyl imide offered high and stable capacity. Furthermore, the electrochemical behavior of a surface film on a lithium metal anode was investigated at various operating temperatures. It was found that the operating temperature during charge/discharge cycling influences the morphology of the film on a lithium metal anode, resulting in the variation in charge/discharge coulombic efficiency of a lithium metal anode. The results are discussed in view of the stability of electrolyte solutions and the film formation between the negative electrode and the organic electrolyte solution. © 1997 Elsevier Science S.A.

Keywords: Rechargeable lithium batteries; Organic electrolytes; Lithium salts

1. Introduction

In the course of the development of lithium (Li) batteries, one of the authors started the research of primary lithium batteries with organic electrolytes in 1967 [1,2]. Since then, the electrolyte solution has been one of most important subjects for the development of primary and secondary lithium batteries. For example, in the field of Li-ion batteries one of the important questions is which electrolyte solution is most suitable for each carbon material as well as each cathode material [3–5]. Generally, an Li metal anode is more reactive than an Li-carbon anode and needs stricter choice of the electrolyte solution. Furthermore, the chemical and physical properties of the film formed via the reaction of the solution with an Li metal anode affects the charge/discharge behavior of an Li metal anode [4,6].

The present paper reports our recent findings on the suitability of the organic electrolyte systems for highly graphitized carbon anodes, focusing on the stability of co-solvents included in ethylene carbonate-based electrolytes and on the stability of Li salts. We also report the electrochemical behavior of a surface film formed on an Li metal anode at various operating temperatures.

2. Suitability of electrolyte solutions for Li–carbon electrodes

In the 1970s and 1980s, the important subjects on electrolyte solutions were conductivity and stability [7]. However, practical Li-ion batteries commercialized in 1991 needed special electrolyte solutions [8,9]. Li-ion batteries need wide potential ranges and excellent cycleability including high capacity and long cycling life. At the present, an essential solvent for Li-ion batteries is ethylene carbonate (EC). For example, the electrolyte solutions using single solvents, i.e., propylene carbonate (PC), butylene carbonate (BC), 4-methyl dioxolane (4-MeDOL), 2-methyl tetrahydrofuran (2MeTHF), dimethoxy ethane (DME) and dimethyl sulfoxide (DMSO), were not suitable for electrochemical Li intercalation into pitch-based carbon fiber (PCF) heat-treated in N_2 atmosphere at 2800°C as shown in Table 1, because PCF was destroyed to powder during charging and, therefore, no discharge capacity was obtained [3]. The destruction of PCF was mainly due to the exfoliation caused by solvent co-intercalation with Li. Details of PCF structural parameters were described elsewhere [3]. PCF had highly graphitized bulk; d_{002}, L_c and L_a were 3.371, 450 and 780 Å, respectively. The texture of the cross section of PCF was radial with fine zigzag layers. The current density was controlled at 30 mA g^{-1} (per mass of PCF), and the potential ranges of PCF were

* Corresponding author.

PII S0378-7753(97)02515-9

Table 1
Electrode properties of PCF in various electrolytes consisting of single solvent

	EC	BL	S	DEC	PC	BC	4-MeDOL	2MeTHF	DME	DMSO
Initial coulombic efficiency (%)	96.4	87.5	34.3	7.7						
Initial capacity (mAh/g)	277	214	22	16	no intercalation					
Maximum capacity (mAh/g)	292	22	16							

Table 2
Electrode properties of PCF in various electrolytes consisting of EC + X(50/50 v/v)

	BL	S	AN	DEC	PC	BC	4MeDOL	2MeTHF	DME	DMSO
Initial coulombic efficiency (%)	94.4	98.8	96.4	96.3	91.0	90.2	89.6	85.8	1.4	1.8
Initial capacity (mAh/g)	288	267	300	289	270	209	287	274	1.8	4.1
Maximum capacity (mAh/g)	289	270	301	304	279	237	290	282	4.1	8.5

0 and 1.0 V versus Li/Li^+; these conditions were applied to all the cycling tests with PCF.

In the case of mixed solvents, EC + co-solvent (X) / 1 M lithium perchlorate ($LiClO_4$), PCF showed high initial efficiency and large discharge capacity except EC + DME and EC + DMSO as listed in Table 2: X = γ-butyrolactone (BL), sulfolane (S), acetonitrile (AN), diethyl carbonate (DEC), PC, BC, 4MeDOL, 2MeTHF, DME or DMSO. Especially in the electrolytes of EC + AN and EC + DEC, PCF showed the same initial discharge efficiency as that in the EC electrolyte (96%), and showed larger initial capacity and larger maximum capacity. The other electrolytes decreased the initial coulombic efficiency compared with that in the EC electrolyte. These changes of initial efficiency dependent on EC + X seemed to show both suitability of X for smooth intercalation of Li into PCF and reactivity of X with Li-intercalated PCF. It was assumed that reactivity of X would be very small in a mixture EC + X to the first approximation because the affinity of EC with Li was stronger than that of the other solvents. Therefore, if the initial efficiency in EC + X is the same as that in EC, as in EC + AN and EC + DEC, suitability of X for smooth intercalation is similar to EC. On the other hand, less efficiency in EC + X than in EC itself seemed to agree with a lower suitability of X for smooth intercalation of Li than in EC. Thus, accounting for the value of the initial coulombic efficiency, the order of suitability for the Li-intercalation reaction was determined as follows: EC > AN, DEC > BL > S > PC > BC, 4MeDOL > 2MeTHF > DME, DMSO.

The influence of the electrolyte solutions on the charge/discharge performance would be caused by co-intercalation with Li^+ into the carbon electrode and film formation on the anode. The composition of the film would be a mixture of lithium halides, lithium carbonate, lithium alkyl carbonates, ethylene di-lithium carbonate $(CH_2OCO_2Li)_2$, lithium alkoxides, lithium oxide, lithium hydroxide, etc. The thickness of the film and the composition are controlled by the solubility of the organic electrolyte solutions [4,6].

3. Lithium salts of the electrolyte solutions

An electrolyte salt is a very important constituent of the electrolyte solution. Recently, the most usual Li salt in the organic electrolyte solutions is lithium hexafluorophosphate ($LiPF_6$) for commercial Li-ion batteries [10]. From a view point of cycling performance and stability, however, lithium trifluoromethanesulfonate ($LiCF_3SO_3$) [11] and lithium bistrifluoromethylsulfonyl imide ($Li(CF_3SO_2)_2N$) [12–17] are interesting salts. Specific conductivities of $LiPF_6$ and $Li(CF_3SO_2)_2N$ are similar, and these are higher than that of $LiCF_3SO_3$ [13,14]. The ion size of $Li(CF_3SO_2)_2N$ is larger than that of PF_6^-, but the conductivity of $(CF_3SO_2)_2N^-$ is high. This high conductivity of $(CF_3SO_2)_2N^-$ is caused by a high dissociation of this salt due to the electronic structure with high resonance [14].

Details of graphitized mesocarbon microbeads (MCMBs) preparation were described elsewhere [18–20]. The resulting MCMBs had highly graphitized bulk; d_{002}, a_0, L_c and L_a were 3.37, 2.46, 460 and 610 Å, respectively [20]. The charge/discharge characteristics of MCMBs were evaluated by galvanostatic cycling at 6 mA g^{-1} (per mass of MCMBs). The cutoff voltages of the charge and the discharge were 0 and 2.0 V, respectively. Fig. 1 displays the voltage–time curves during first and second charge/discharge cycles of coin-type cells with MCMBs electrode and EC-based electrolytes containing 1 M $Li(CF_3SO_2)_2N$; DMC and MP note dimethyl carbonate and methyl propionate, respectively. At the first charging in each EC-based electrolyte system, the voltage gradually decreased to reach ~0.25 V, and then a long plateau was observed to 0 V. At the second charging cycle in each electrolyte system, the portion of the curve in the high voltage region (> 0.25 V) became shorter, and the plateau remained long to 0 V. On the other hand, the profiles of discharge curve observed at first and second cycles in each system were essentially similar in a long plateau from 0 to 0.25 V and in abrupt increase to 2.0 V. In each system a considerable difference between the charge and discharge

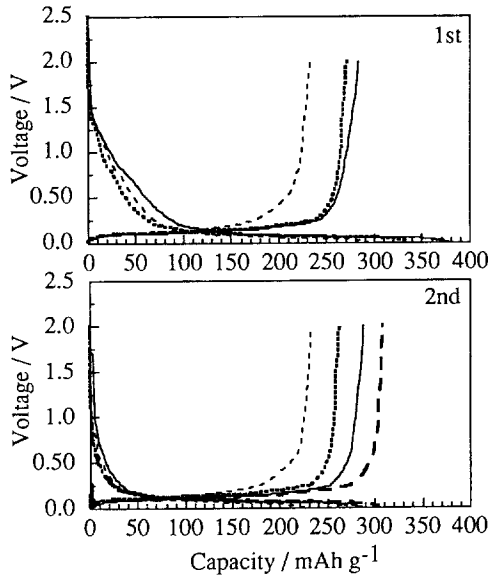

Fig. 1. First and second charge/discharge curves of the coin-type cells with MCMBs electrode; electrolytes: (——) EC-DME; (— — —) EC + DMC; (— — —) EC + DEC, and (- - -) EC + MP containing 1 M $Li(CF_3SO_2)_2N$.

capacity, 'irreversible capacity', was observed during the first cycle. The irreversible capacity was hardly observed after the first cycle in each electrolyte systems. The irreversible capacity at the first cycle as well as the above-mentioned profiles of the charging and discharging curves is typical for highly graphitized carbon electrodes used in rechargeable lithium batteries [14–18]. The irreversible capacity ascribed to the decomposition of electrolyte components at the first charge process and/or to lithium remaining in host carbon at the first discharge process is known to be inevitable in most carbon systems [18–22]. If the irreversible capacity during the first cycle does not induce the degradation of the charge/discharge capacity and cycleability in the following cycles, it will do no harm [4]. It often happens that the film resulting from the decomposition of the electrolyte on the surface of the electrode during charging covers and inactivates carbon's active sites inducing undesirable side reactions [4].

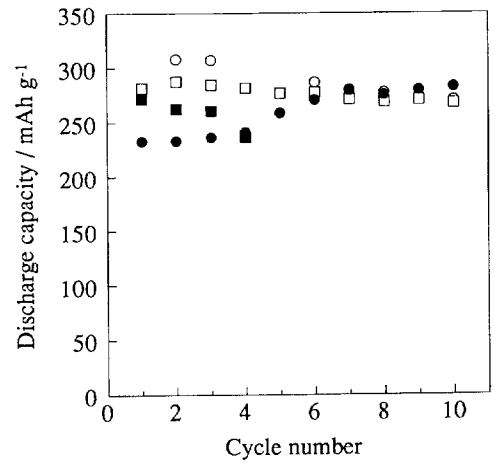

Fig. 2. Cycle dependence of discharge capacity of the coin-type cells with MCMBs electrode; electrolytes: (○) EC + DME; (□) EC + DMC; (●) EC + DEC, and (■) EC + MP containing 1 M $Li(CF_3SO_2)_2N$.

The cycle dependence of the discharge capacity of the MCMBs electrode was observed using the coin-type cells with EC-based electrolytes as shown in Fig. 2. In the case of the EC + DMC electrolyte system, the discharge capacity was almost stable during cycling, while the discharge capacities in the other EC-based systems fluctuated until ~ sixth cycle to reach the same capacity as the EC + DMC system (270–280 mAh g^{-1}). It was reported that the maximum discharge capacity of MCMBs graphitized at 2800°C was estimated to be 282 mAh g^{-1}, taking into account the existence of turbostratic structure between the graphite layers of the graphitized MCMBs [20]. $Li(CF_3SO_2)_2N$ is, therefore, regarded as one of most attractive electrolytic salts for highly graphitized carbon electrodes such as MCMBs graphitized at 2800°C because it guarantees stable discharge capacity nearly equal to 'maximum capacity' even at repeated cycling. Except for the first cycle the coulombic efficiency of each charge/discharge cycle was estimated to be almost 100% in every electrolyte systems.

In order to obtain interfacial characteristics between the MCMBs electrode and the electrolytes during charging, a.c. impedance measurements of the electrode were carried out. Figs. 3 and 4 show Cole–Cole plots observed before and during charging the MCMBs electrode at each potential in the EC + DMC and EC + DEC systems, respectively. An arc

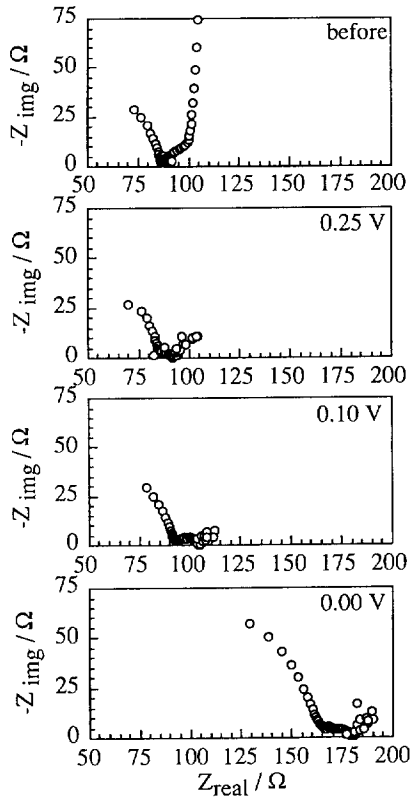

Fig. 3. Cole–Cole plots observed before and during charging MCMBs electrode at each potential (0.25, 0.10 V and 0.00 V vs. Li/Li^+) in EC + DMC containing 1 M $Li(CF_3SO_2)_2N$.

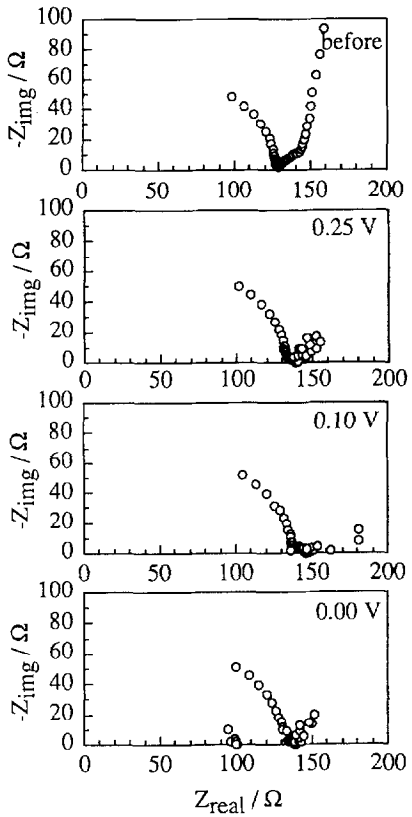

Fig. 4. Cole–Cole plots observed before and during charging MCMBs electrode at each potential (0.25, 0.10 V and 0.00 V vs. Li/Li^+) in EC + DEC containing 1 M $Li(CF_3SO_2)_2N$.

appearing in the high frequency region (corresponding to the left part of profiles) should be due to charge-transfer process between the Li ion and the host carbon and not be due to the film derived from the decomposition of electrolytes at the interface during charging, because the arc was observed even before charging. No change in the shape of the arc in the high frequency region was observed in the electrolyte systems except the EC + DMC system at 0 V during charging. The arcs observed until 0.1 V in the EC + DEC system were somewhat larger than the arcs in the EC + DMC system, suggesting the interfacial resistance in the EC + DEC system was larger than that in the EC + DMC system. The difference in resistance between two systems at the first charging would be correlated with the difference of the first discharge capacity between the corresponding systems as shown in Figs. 1 and 2. Therefore, the abrupt increase of the arc at 0 V in the EC + DMC system would be due to the variation in the charge-transfer resistance with the abundant storage of Li ion in the host MCMBs and with the resulting change of the stage structure [21]. It is notable that the appearance of new arc ascribed to the film formation in the Cole–Cole plots can be hardly observed during charging to the negative potential. On the other hand, the film formation obviously detectable by the a.c. impedance analysis (in this case, therefore, the film has high resistance) at the first charging has been reported in most electrolyte systems containing $LiPF_6$; the film formation has been usually observed below ~ 1 V during the first charging on the surface of the highly graphitized carbon electrodes [4,21,22]. Even if the film was formed during the first charging process in the electrolyte containing $Li(CF_3SO_2)_2N$, the film resistance was low, judging from a.c. impedance response observed in Figs. 3 and 4. Thus, in the $Li(CF_3SO_2)_2N$ systems the irreversible capacity at the first cycle shown in Fig. 1 should not contribute to the film formation inducing the degradation of the discharge capacity.

$Li(CF_3SO_2)_2N$, lithium imide, provides stable interface between the MCMBs electrode and the electrolytes during charging. This desirable property would be correlated with stable and excellent charge/discharge performance of the MCMBs electrode in the EC-based electrolytes containing $Li(CF_3SO_2)_2N$. On the other hand, however, a shortcoming of $Li(CF_3SO_2)_2N$ as well as $LiCF_3SO_3$ is their cathodic stability; e.g., $Li(CF_3SO_2)_2N$ reacts with the aluminum current collectors used for most cathode materials [23]. In order to overcome this drawback, a novel salt, lithium tris(trifluoromethanesulfonyl)methide [$LiC(CF_3SO_2)_3$], has been investigated [23,24]. The reported cathodic stability of this salt is excellent [23,24]. The further investigation on the anodic behavior of this salt is desired.

4. Temperature effect on the behavior of Li metal anodes

The film formation and dissolution on the interface between the anode and electrolyte solution are very important factors for the performance of the anode as mentioned in a previous section. For example, in a recent paper, methyl acetate, methyl propionate and ethyl propionate showed excellent properties as the co-solvent for Li-ion batteries [25]. These effect of co-solvents on the anode performance would be closely related with the difference in solubility of the resulting film from the co-solvent on the electrode.

The film formation and dissolution are influenced by temperature [26]. Fig. 5 shows the Cole–Cole plots of the impedance at an Li electrode in EC + DMC/1 M $LiCF_3SO_3$ with charge/discharge cycling at various temperatures; both the charge and discharge currents were 0.5 mA cm^{-2}, the charged electricity was 0.1 C cm^{-2}, and the cutoff voltage for discharge was 1.5 V versus Li/Li^+. This charge/discharge technique was described in detail elsewhere [27–29]. The observed impedance responses may essentially consist of triple quasi-semicircles as shown in Fig. 6. We assumed that these responses are equivalent to the triple connection in series of a parallel combination of a capacitance and a resistance. In the overall circuit, R_S is the resistance related mainly to the electrolyte resistance. C_n and R_n ($n = 1$, 2 and 3) are the capacitance and the resistance in each parallel component, respectively; the numeric (n) is in the order of the frequency (from the higher frequency region to the lower one). Such triple semicircle response would be attributed to the multi (double or triple)-layer films with different chemical components on the Li anode [30]. The overall resistance of the

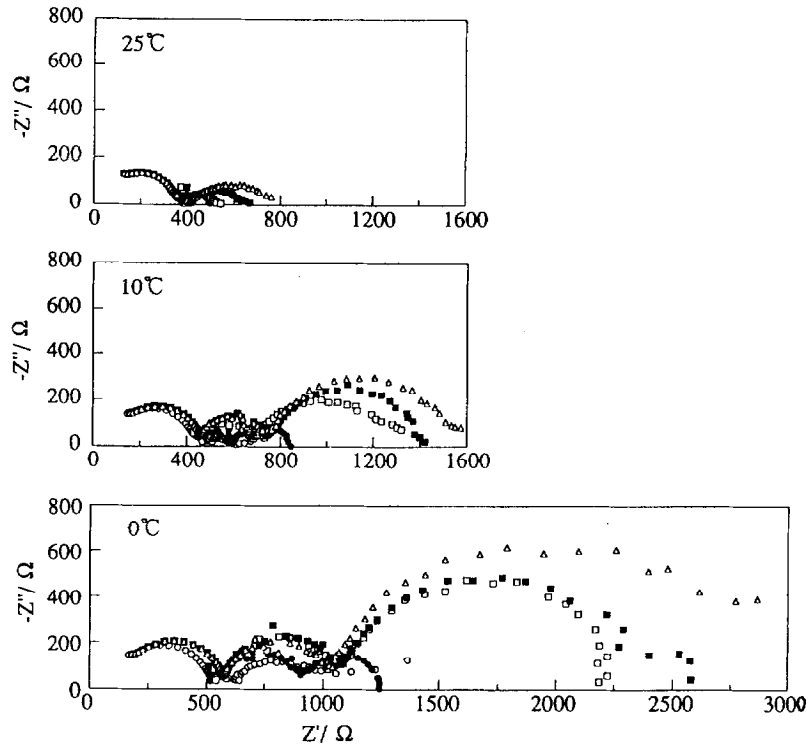

Fig. 5. Cole–Cole plots of the impedance at the Li electrode in EC + DMC containing 1 M $LiCF_3SO_3$ at various temperatures with cycle number: (○) first cycle; (●) fifth cycle; (□) 10th cycle; (■) 15th cycle, and (△) 20th cycle.

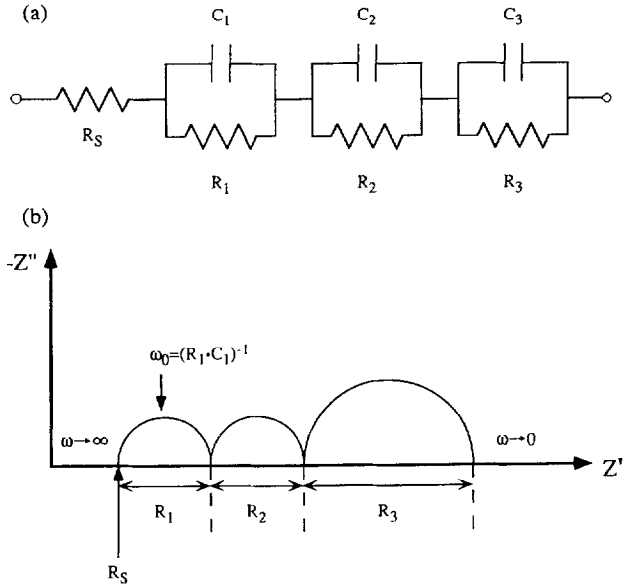

Fig. 6. Impedance model at the interface of the Li anode in EC + DMC containing 1 M $LiCF_3SO_3$, equivalent (a) the electrical circuit, and (b) the corresponding impedance diagram.

interface of the electrode increased with a decrease in operating temperature. The separation of the triple quasi-semicircles in the impedance responses in Fig. 5 was distinctly observed when the operating temperature was decreased, suggesting that a well-ordered multi-layer structure was established at low temperature. In addition, the shape of the semicircle in the lower frequency region was observed to be flat at higher temperatures, probably because of the less chemical and morphological homogeneity of each film in the layered structure at the higher temperature [31,32]. These results suggests that at low temperature a well-ordered multilayer structure consisting of the compact and homogeneous films with high resistance would be formed on deposited Li.

Each impedance response observed in the higher, middle and lower frequency regions was individually analyzed in an attempt to characterize the details of the layered film structure. Fig. 7 shows the variations of R_n calculated from the size of the semicircles in each frequency region at various temperatures as a function of the cycle number. No change in the R_1 value at each temperature was observed during cycling. On the other hand, both the R_2 and R_3 values at each temperature increased during cycling. However, the dependency of R_2 and R_3 on cycle number was different. R_2 at each temperature increased until the 10–15th cycle and reached a constant value, while R_3 increased continuously with cycling. Fig. 8 displays the variations of the time constant, the product $R_n \cdot C_n$, in each frequency region at various temperatures with cycle number. The $R_1 \cdot C_1$ values were constant during cycling, while both the $R_2 \cdot C_2$ and $R_3 \cdot C_3$ values varied with cycling except $R_2 \cdot C_2$ at 25°C. On the basis of the cycling behavior of R_n as well as $R_n \cdot C_n$ ($n = 1$–3), each response can be interpreted as follows. The impedance response in the higher frequency region (corresponding to $n = 1$) at each temperature would be ascribed to the charge-transfer process, judging from the constancy of R_1 as well as $R_1 \cdot C_1$ with cycling. The responses in middle ($n = 2$) and lower ($n = 3$) frequency region at each temperature would be due to the surface films on deposited Li because R_2 and R_3 as well as

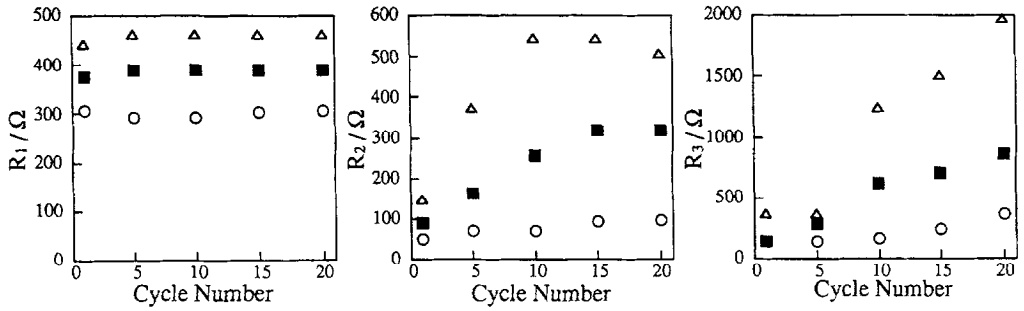

Fig. 7. Variation of R_n with cycle number in EC + DMC containing 1 M $LiCF_3SO_3$ at various temperatures: (○) 25°C; (■) 10°C, and (△) 0°C.

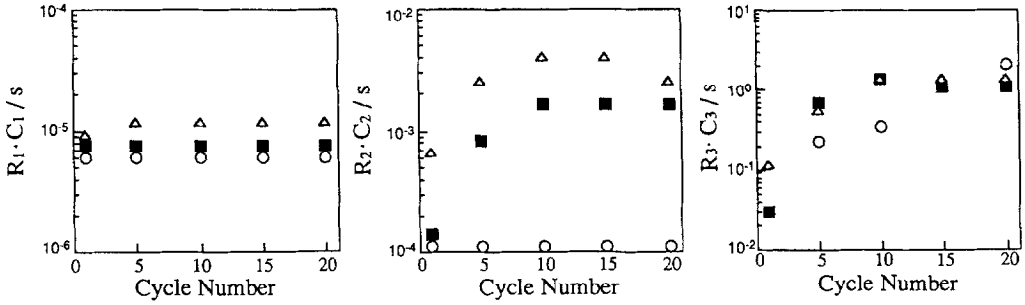

Fig. 8. Variation of $R_n \cdot C_n$ with cycle number in EC + DMC containing 1 M $LiCF_3SO_3$ at various temperatures: (○) 25°C; (■) 10°C, and (△) 0°C.

$R_2 \cdot C_2$ and $R_3 \cdot C_3$ varied with cycling. The response in the middle region and that in the lower region may be attributed to the inner and outer film layers, respectively, taking into account the continuous increase of R_3 throughout cycling and the limited increase of R_2 with initial cycling [30]. In addition, the values of C_1, C_2 and C_3 were estimated to be the order of 10^{-8}, 10^{-6} and 10^{-3} F, respectively. The C_1 value is well consistent with the reported capacitance value of charge-transfer process, and C_2 as well as C_3 value agrees with the reported capacitance values of the film component [30,33]. The remarkable difference between the C_2 and C_3 value may be mainly ascribed to the variation of the film thickness [30]; the inner surface film related to C_2 would be thicker than the outer surface film corresponding to C_3.

The charge/discharge coulombic efficiency tests were performed at various temperatures in an attempt to understand the relationship between the coulombic efficiency and the surface film characteristics at various temperatures. Fig. 9 shows the variations of the coulombic efficiency with cycling in EC + DMC/1 M $LiCF_3SO_3$ at various temperatures; the charge/discharge condition was identical to that applied to the impedance measurement. The efficiency increased with a decrease in temperature. At the low temperature, the compact films would be formed on the deposited Li as mentioned above. This dense films on the Li anode would contribute to the higher coulombic efficiency at the low temperature; the compact solid electrolyte interface, the compact SEI, would suppress the dendritic Li deposition that causes the lowering of the coulombic efficiency in the charge/discharge cycles.

On the basis of the above results and discussion, the characteristics of the Li electrode interface in the applied electrolyte at the higher and lower temperature are summarized as

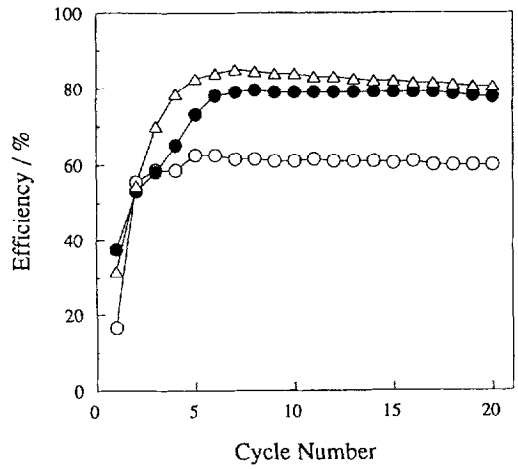

Fig. 9. Variation of the charge/discharge coulombic efficiency of the Li anode with cycle number in EC + DMC containing 1 M $LiCF_3SO_3$ at various temperatures: (○) 25°C; (●) 10°C, and (△) 0°C.

follows. There may be the outer thin film and the inner thick film on the Li surface at each temperature. At the higher temperature, the films would be chemically and morphologically irregular as well as loose (maybe porous). The dendritic deposition of Li may occur, therefore, leading to the low cycling efficiency. On the other hand, at the lower temperature, the compact and homogeneous films may form well-ordered multi-layer structure on the Li surface, resulting in the suppression of the Li dendrite formation to improve the cycling efficiency. The characteristics of the resulting surface films would be governed by the film formation process as well as the solubility of the films; these factors should be much controlled by temperature.

5. Future Prospects

The research subjects of electrolyte solutions of Li batteries started on the conductance and stability. The cycleability and potential window attracted researchers' interest. At the present, film formation on the electrode surface and its control are the main subjects. At a next stage of the development of rechargeable Li batteries, suitable interface structure between the electrolyte and the electrodes shall be designed.

Acknowledgements

The authors thank Dr T. Iijima, Mr H. Kamohara and Miss Y. Takaki for their contribution.

References

[1] H. Tamura, Y. Matsuda and T. Inoue, *22nd Meet. Chem. Soc, Jpn., Tokyo, 1969.*
[2] Y. Matsuda, T. Inoue, H. Yoneyama and H. Tamura, *Kogyo Kagaku Zasshi, 74* (1971) 2205.
[3] T. Iijima, K. Suzuki and Y. Matsuda, *Synth. Met., 73* (1995) 9.
[4] D. Aurbach, Y. Ein-Eli, B. Markovsky, A. Zaban, S. Luski, Y. Carmeli and H. Yamin, *J. Electrochem. Soc., 142* (1995) 2882.
[5] M. Morita, T. Ichimura, M. Ishikawa and Y. Matsuda, *J. Electrochem. Soc., 143* (1996) L26.
[6] D. Aurbach, A. Zaban, A. Schechter, Y. Ein-Eli, E. Zinigrad and B. Markovsky, *J. Electrochem. Soc., 142* (1995) 2873.
[7] Y. Matsuda, *J. Power Sources, 20* (1987) 19.
[8] E. Mashiko, M. Yokokawa and T. Nagaura, *Ext. Abst., 32nd Battery Symp. Jpn., Kyoto, 1991*, p. 31.
[9] M. Nagamine, H. Kato and Y. Nishi, *Ext. Abst., 33rd Battery Symp. Jpn., Tokyo, 1992*, p. 83.
[10] T. Nagaura and T. Tozawa, *Prog. Battery Solar Cells, 9* (1990) 20.
[11] M. Ishikawa, M. Morita, M. Asao and Y. Matsuda, *J. Electrochem. Soc., 141* (1994) 1105.
[12] M. Ishikawa, H. Kamohara, M. Morita and Y. Matsuda, *J. Power Sources*, in press.
[13] L.A. Dominey, J.L. Goldman, V.R. Koch and C. Nanjundiah in S. Subbareo, V.R. Koch, B.B. Owens and W.H. Smyl (eds.), *Proc. Symp. Rechargeable Lithium Batteries*, Hollywood, FL, Proc. Vol. 90-5, The Electrochemical Society, Pennington, NJ, USA, 1990, p. 56.
[14] A. Webber, *J. Electrochem. Soc., 138* (1991) 2586.
[15] T.D. Tran, J.H. Feikert, X. Song and K. Kinoshita, *J. Electrochem. Soc., 142* (1995) 3297.
[16] M. Odziemkowski and D.E. Irish, *J. Electrochem. Soc., 140* (1993) 1546.
[17] A.M. Wilson and J.R. Dahn, *J. Electrochem. Soc., 142* (1995) 326.
[18] K. Tatsumi, N. Iwashita, H. Sakaebe, H. Shioyama, S. Higuchi, A. Mabuchi and H. Fujimoto, *J. Electrochem. Soc., 142* (1995) 716.
[19] A. Mabuchi, K. Tokumitsu, H. Fujimoto and T. Kasuh, *J. Electrochem. Soc., 142* (1995) 1041.
[20] A. Mabuchi, H. Fujimoto, K. Tokumitsu and T. Kasuh, *J. Electrochem. Soc., 142* (1995) 3049.
[21] N. Takami, A. Satoh, M. Hara and T. Ohsaki, *J. Electrochem. Soc., 142* (1995) 371.
[22] N. Takami, A. Satoh, M. Hara and T. Ohsaki, *J. Electrochem. Soc., 142* (1995) 2564.
[23] E. Croce, A. D'Aprano, C. Nanjundiah, V.R. Koch, C.W. Walker and M. Salomon, *J. Electrochem. Soc., 143* (1996) 154.
[24] C.W. Walker, J.D. Cox and M. Salomon, *J. Electrochem. Soc., 143* (1996) L80.
[25] A. Ohta, H. Koshina, H. Okuno and H. Murai, *J. Power Sources, 54* (1995) 6.
[26] M. Ishikawa, Y. Takaki, M. Morita and Y. Matsuda, to be published.
[27] V.R. Koch and S.B. Brummer, *Electrochim. Acta, 23* (1978) 55.
[28] Y. Matsuda, M. Ishikawa, S. Yoshitake and M. Morita, *J. Power Sources, 55* (1995) 301.
[29] M. Ishikawa, K. Otani, M. Morita and Y. Matsuda, *Electrochim. Acta, 41* (1996) 1253.
[30] N. Takami, T. Ohsaki and K. Inada, *J. Electrochem. Soc., 139* (1992) 1849.
[31] J.G. Thevenin and R.H. Muller, *J. Electrochem. Soc., 134* (1987) 273.
[32] M. Morita, S. Aoki and Y. Matsuda, *Electrochim. Acta, 37* (1992) 119.
[33] S. Morzilli, F. Bonino and B. Scrosati, *Electrochim, Acta, 32* (1987) 961.